OBSERVATIONS OF WATER MOVEMENT IN A BLOCK OF FRACTURED WELDED TUFF

Falah Thamir
U.S. Geological Survey
Box 25046, MS 421
Denver, CO 80225
(303) 236-5189

Edward M. Kwicklis
U.S. Geological Survey
Box 25046, MS 421
Denver, CO 80225
(303) 236-6228

David Hampson
Foothills Eng. Cons., Inc.
350 Indiana St., No. 415
Golden, CO 80401
(303) 236-0408

Steve Anderton
ROCKTECH
7494 Platinum Circle
West Jordan, UT 84084
(801) 255-5222

ABSTRACT

A laboratory water infiltration experiment through a block of fractured, moderately welded volcanic tuff was conducted at different boundary pressures. The block measured 47.5 cm long x 54.3 cm wide x 80.6 cm high. The purpose of the experiment was: (a) to test an instrumentation scheme for a field test, and (b) to make flow measurements through a fractured network at different boundary pressures to understand mechanisms that affect fracture flow. The upper boundary water pressure was decreased in steps; each step lasted several weeks where the pressure was kept steady. Water inflow and outflow rates were measured for each boundary condition. Entrapped air was found to impede water movement. The gas phase in the fracture network was found to not be continuous; its pressure within the network was not known. The matric potential values could not be measured with tensiometers alone since a known gas pressure is required. Long-term input and output flow rates were equal. Outflow rate did not stabilize during the test period; it continued to decrease, even when the upper boundary water pressure was kept steady. No relation between boundary pressure and flow rate was established. Bacteria, which was found in the outflow, possibly caused variations in the behavior. Trapped air caused the outflow to periodically decrease or stop; however, outflow rates following the interruptions did not change long-term flow trends.

I. INTRODUCTION

Studies are being conducted in the United States at the Yucca Mountain area in Nevada to evaluate the suitability of the site as a mined geological repository for disposal of high-level radioactive nuclear waste. The thick unsaturated zone surrounding the potential repository is being studied to determine if it will be a barrier for water movement to the accessible environment at the proposed site.

One of several proposed onsite tests that will be done to characterize the unsaturated zone is the Percolation Test in the Exploratory Studies Facility at Yucca Mountain[1]; its purpose is to gather field data that can be used to verify and validate conceptual and numerical models of fluid flow and solute transport through variably-saturated and fractured tuff. The planned approach to the field test is to make water-flow measurements through blocks of volcanic tuff with well-characterized properties and controllable boundary conditions. The observed flow rates will be compared with modeled rates; the comparison will be used to evaluate the accuracy of models utilized to predict long-term behavior of larger scales not amenable to direct testing.

In preparation for the field test, a prototype laboratory experiment was conducted on a block of welded tuff. The purpose of the experiment was to ascertain the feasibility of monitoring and characterizing liquid water percolation and tracer movement in fractured rock, and find an appropriate design of the field apparatus to measure liquid flow rate and pressure at different boundary conditions. To achieve these goals, a system with controllable boundary pressure and flow rate was designed and successfully implemented in the laboratory[2]; preliminary data were published. The system will be implemented in the planned field experiment[1]. In this paper, additional measurements that followed the publication of the first report[2] are presented; they include water pressure distribution within the fractures and matrix, and water inflow and outflow rates under unsaturated conditions. These measurements will be used to help understand mechanisms that affect unsaturated fluid flow in fractured rock.

DISCLAIMER

Portions of this document may be illegible in electronic image products. Images are produced from the best available original document.

II. EXPERIMENTAL DESIGN

A block of fractured, moderately welded tuff, 47.5 cm long x 54.3 cm wide x 80.6 cm high, was cut from a boulder retrieved from an outcrop of the Tiva Canyon Member of the Paintbrush Tuff. Some of the matrix physical properties were estimated from core samples taken from trimmed portions of the boulder from which the block was cut (Table 1). The variability in permeability measurement did not indicate the existence of directional dependence. The block had two major fractures (F1 and F5 in Figure 1) with several other minor fractures.

Table 1 - Block-matrix properties
[cm = centimeter; g = gram; L = liter; m = meter; s = second]

Sample Direction	Porosity	Permeability, m^2 (x 10^{-18})	darcy (x 10^{-6})	Hydraulic Conductivity, m/s (x 10^{-12})
vertical	0.064	3.060	3.100	30.0
vertical	0.059	0.182	0.184	1.78
horizontal	0.063	0.810	0.821	7.93
horizontal*	0.064	5.160	5.230	50.5
average	0.0625	2.303	2.334	22.5
std	0.0024	2.270	2.301	22.2

Other Block Properties:
Size: 47.5 cm long x 54.3 cm wide x 80.6 cm long
Total pore volume = 13.0 L; std = 0.48 L
Average bulk density = 2.25 g/cm³; std = 0.064 g/cm³
Average grain density = 2.40 g/cm³; std = 0.071 g/cm³

* The two horizontal samples were taken in the same direction.

Eighteen 12.7-mm diameter holes were drilled such that some intersected fractures and some went through rock matrix only (Figure 1). Holes 2B, 3B, 3C, 3D, 4C, and 4D were matrix holes; the rest intersected fractures. This drilling scheme was chosen so that water pressure in the fractures and matrix can be monitored.

Following borehole drilling, the block was placed on a frame such that all sides were accessible for instrumentation, including the top and bottom (Figure 2). The block was encased in an acrylic enclosure to minimize evaporation and to maintain stable boundary conditions. Two layers of sorted, prewashed Ottawa sand were placed along the block bottom and top. The top sand layer was isolated from the annular space surrounding the block with an additional acrylic enclosure (Figure 2). The sand layers were placed to evenly distribute the water along both ends of the block. The top sand layer was also used to mimic the hydraulic interaction between fractured welded tuff and

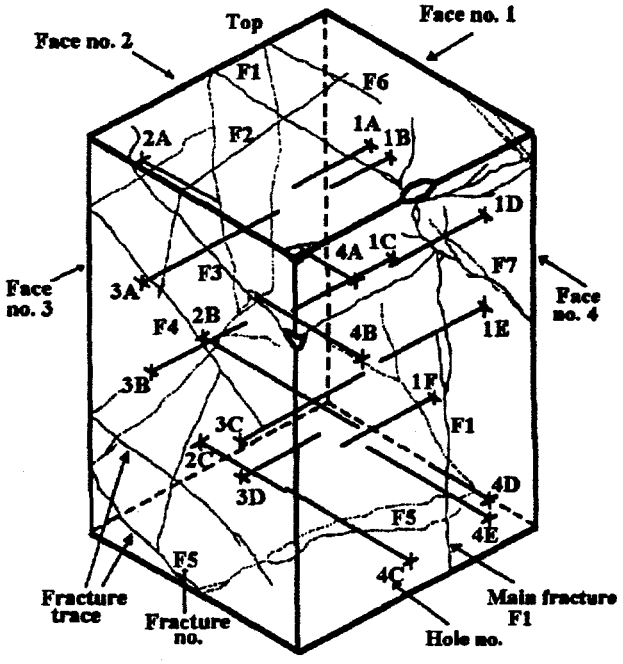

Figure 1 - A diagram of the block showing fracture traces and boreholes.

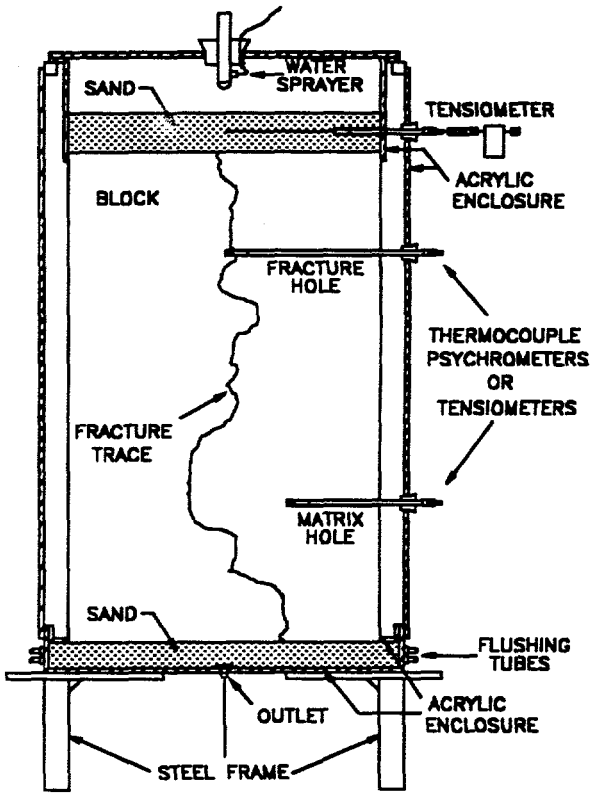

Figure 2 - Experimental setup of the block showing the frame, enclosure, sand layers, and instruments.

more porous and permeable tuff or alluvium layers. The diameter of the sand grains ranged between 100 and 500 μm. Table 2 lists the geometry and some properties of both sand layers. Figure 3 shows the matric-potential water-saturation relation of sand samples with an initial bulk density of 1.70 g/cm^3, which is close to the bulk densities of the lower and upper (final) sand layers. The second cycle shown in Figure 3 represents the block sand layers more realistically; the first cycle usually is accompanied by structural changes in the sand after wetting, resulting in more compact sand grains, as indicated in Figure 3. The final bulk density of the upper sand layer is the density attained after compaction took place following the addition of water (Table 2). The annular space around the block was isolated from the lower sand layer using acrylic strips and silicone rubber sealant. The seal was tested and withstood 10 kPa of air pressure. Isolation of the lower sand layer from the annular space allowed fluid pressure in the sand to be independently controlled or measured during the experiment.

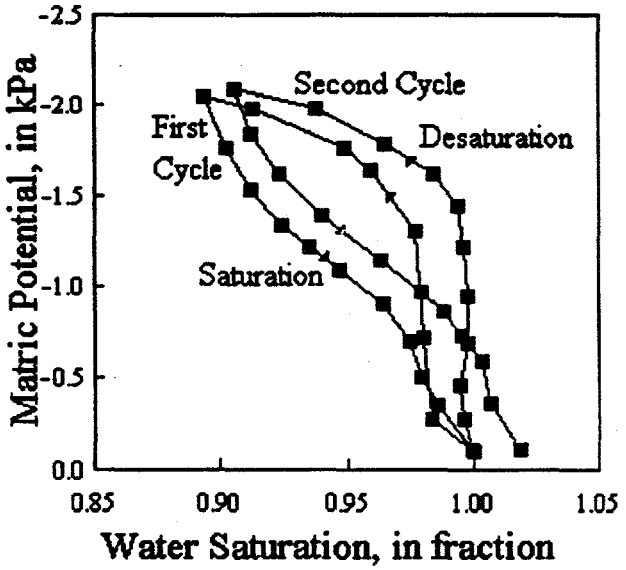

Figure 3 - Matric potential-water saturation relation of the upper and lower sand layers.

Probes for thermocouple psychrometers or tensiometers were constructed to measure water and matric potentials[2]. Rubber packers were used to isolate the sensors within a desired section in a hole. The psychrometers were used to measure water potentials ranging between -7000 and -100 kPa. The tensiometers were used to measure matric potentials greater than -85 kPa. Atmospheric pressure was used as the reference pressure for the tensiometers.

To achieve the objectives of this prototype test, it was necessary to have an interconnected network of fractures so that water could flow through it. Before starting the test, cross-hole gas-injection was used to determine and verify the interconnectedness of the fracture network within the block. Nitrogen was repeatedly injected through holes that intersected fractures using packer gas-injection probes[2]; pressure was monitored in several surrounding holes. The main fracture (F1 in Figure 1) was permeable to air between hole 3A (close to the top of the block), and monitoring holes 1F and 4E (close to the bottom of the block); hole 1F intersects fracture F1 or F5 and hole 4E intersects fracture F5. After three initial testing stages were completed[2], cross-hole gas-injection was repeated while there was water above and around the lower part of the block. Air bubbles were observed coming out of the top and bottom simultaneously, verifying a continuous path from top to bottom.

Table 2 - Properties of the upper and lower sand layers
[mm= millimeter; g= gram; L=liter; i= initial; f= final]

Sand Layer	Thick-ness, mm	Bulk Density, g/cm^3	Porosity, fraction	Pore Volume, L
UPPER$_i$	102	1.57	0.41	11.0
UPPER$_f$	94	1.70	0.36	8.9
LOWER	32	1.74	0.34	3.9

III. EXPERIMENTAL PROCEDURE

The experiment was conducted in a laboratory at room temperatures between 22 and 26 °C. The block was initially air-dry. Testing went through six stages (Table 3). The initial three stages were discussed in a previous paper[2] and will be briefly reviewed. The subsequent three stages will be discussed in this paper.

A. Initial Testing Stages

Two tensiometers were placed in the upper sand layer at 5 cm above the sand-rock interface to measure the water pressure along the top boundary (Figure 2). Water was added in pulses at the beginning of the first and second stages. During the third stage, water was continuously added to maintain constant values of water pressure in the upper sand layer[2]. Thermocouple psychrometers were initially installed in all holes; they were successively replaced with tensiometers as the water potential in the block reached the psychrometer upper measurement limit (-100 kPa).

The first two stages together lasted 187 days; water pressure was kept negative in the upper sand layer most of the time; no water was observed coming out of the block bottom. The third stage was initiated to establish a

Table 3 - Testing stages, tracers, and water amount used during the experiment [cont. = continuous; L = liters; NA = Not Applicable; elapsed time since T_0; Elapsed Time is to beginning of stage]

Stage No.	Starting Date	Elapsed Time, days	Tracer Type	Concentration, ppm	Water Amount, L
1	05-Nov-91	11	Bromide (Br^-)	30	10.0
2	13-Feb-92	111	Iodide (I^-)	20	3.2
3	11-May-92	198	Boron (B^{+3})	20	cont.
4	26-Jan- 93	458	none	NA	0.0
5	01-Jul - 93	614	none	NA	0.0
6	13-Sep- 93	688	*m*-TFMBA	20	cont.

relationship between water flow rate through the block and boundary pressure values at both negative and positive values; it lasted 260 days. At the beginning of the third stage, water pressure in the upper sand layer was kept negative; no significant flow rates into the block were observed. Subsequently, the upper boundary pressure was gradually increased until it reached positive values indicated by ponded water on top of the upper sand layer. When the top pressure became positive, measurable flow rates into the block were achieved (Table 4). Figure 4 shows a record of measured inflow rates when water pressure was positive. Inflow rates were intermittent and sporadic, especially towards the end of stage 3 (Figure 4). No water was observed in the bottom sand layer. Towards the end of the third stage (days 380 to 438 in Figure 4), flow into the block occurred with more frequency and higher rates. However, during the last 20 days of the third stage (days 438 to 458 in Figure 4), no measurable inflow rate was recorded. Consequently, the experiment was terminated, and data collection was stopped. The ponded water was left on top of the block at 38 mm above the sand layer.

Although water flow rate into the block was sporadic during the third stage, the block matrix continued to imbibe water. Imbibition was verified from thermocouple psychrometer readings which indicated a long-term increase in water potential (Figure 5). The apparent decrease in water potential in hole 1D after day 430 is questionable because psychrometers are not accurate above -100 kPa. No explanation was found for the sudden changes in water potential about day 422.

Towards the end of the third stage, some biological growth was seen on the block along the sides, although formaldehyde (HCHO) at 200 ppm (by mass) and calcium selenate ($CaSeO_4$) at 0.0065 molal were added to the water and used as bactericides during the first three stages[2]. This observation is not unusual since biological activity in porous media is known to continue even with the most effective water treatments[3].

Table 4 - Water flow rate into the block at different water pressure values [cm = centimeter; var. = variable; water pressure values at upper sand-rock interface; elapsed time since T_0]

Water Pressure, kPa	Starting Date	Elapsed Time, days	Water Flow Rate, cm^3/day Input	Output
+1.00	11-May-92	198	100 down to 50	0
+1.05	18-May- 92	205	50 down to 30	0
+1.20	07- Jul - 92	256	see Figure 4	0
+1.40	02-Nov -92	373	see Figure 4	0
+1.40[a]	26- Jan -93	458	not measured[b]	0[c]
<+1.40[d]	01- Jul -93	614	not measured	not measured
var.	13- Sep- 93	688	see Figure 8	see Figure 8

Notes:
a. Initial water pressure; water was left on the top of the block; water level dropped slowly during this period to about 1.3 kPa.
b. No data collected.
c. No water observed coming out of the block.
d. Period began when gas injection started. Water pressure was positive during most of this period; it dropped to about 1.2 kPa, then suddenly water drained through the block at the end of this period.

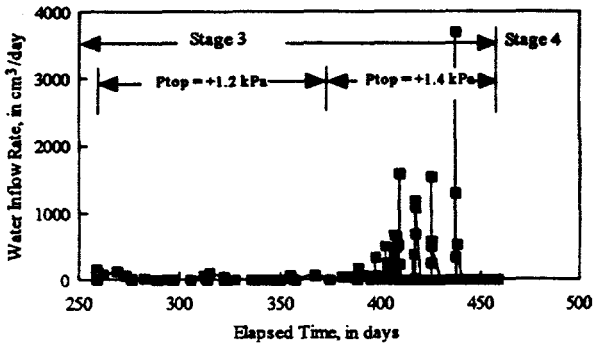

Figure 4 - Water flow rate into the block during stage 3 at different upper boundary pressures [P_{top} = pressure along top rock-sand interface].

B. Final Testing Stages

During the fourth stage, which lasted 156 days, no data were collected; no noticeable decrease in the water level above the block was observed. Biological growth continued to exist along the block exterior.

The fifth stage was a gas injection stage conducted to estimate gas permeability of some of the fractures, and to verify continuity of the fractures after the test was initially terminated at the end of stage 3. The bottom sand layer

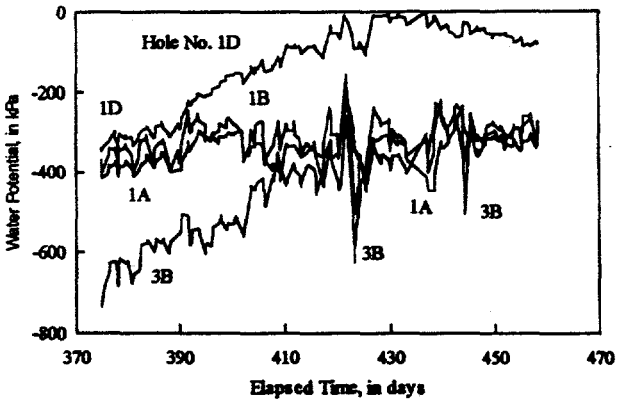

Figure 5 - Water potential measurements within the block from thermocouple psychrometers at the end of stage 3.

looked dry when observed from the bottom acrylic window prior to starting this stage. When gas injection started through hole 3A, water started coming out of fracture F1 along the top third of faces no. 2 and no. 4, and fracture F5 along the bottom of face no. 1; this indicated the existence of water in the fractures. When gas injection continued, bubbling along the sides gradually decreased, then stopped, although gas continued coming out of the fracture traces; this indicated that fractures were dewatering during gas injection. When injection was resumed after being halted for at least 12 hours, bubbling resumed from the same locations that dewatered from the previous gas injection test, indicating that water was continuously moving within the fractures; the source of this water is unknown. Gas injection was done intermittently over a 27-day period. The water coming out of the fractures was analyzed for bacterial content and was found to contain at least 1,000,000 CFU/cm^3; the water in the annulus had at least 900,000 CFU/cm^3; the water in the upper sand layer had at least 50,000 CFU/cm^3; the species were not identified. Nutrients for bacterial growth were expected to exist in the block since it was cut from a boulder that was retrieved from an outcrop that was exposed to biological activity at the surface.

While gas injection was being conducted, simultaneous bubbling was observed coming out of the top and bottom of the block through fractures F1 and F5. The top bubbling was through the water left on top of the block. The bottom bubbling was observed when a seal along the bottom that isolates the lower sand layer from the annulus broke due to the pressure buildup in the bottom sand layer while the bottom outlet valve was shut during gas injection; the bubbling was through some water that had accumulated in the annulus. The simultaneous bubbling confirmed that fractures F1 and F5 were indeed continuous throughout the block. Fracture F6 also bubbled along its top trace, indicating that it was interconnected with fracture F1.

The bottom sand layer started to wet one day after gas injection started; twenty days later it appeared completely wet. During this period the top water level fell approximately 13 mm which is equivalent to 3.4 L of water. The pore volume of the lower sand layer is 3.9 L (Table 2). Although the bottom sand layer appeared completely wet, it was not expected to become fully saturated since air usually becomes trapped when displaced by water in a porous medium.

Forty-six days after gas injection started and 20 days after the last gas injection test was done, the ponded water that remained on top of the upper sand layer suddenly drained. Some of the water accumulated in the annulus and some in the flushing tubes that surround the bottom sand bed. Drainage occurred during a three-day period and was not observed nor recorded because it happened while no data collection was taking place. For the next 15 days, water continued to drain from the upper sand layer through the block. After this incident was observed, measurements similar to those made during the third stage were resumed.

The sixth stage was initiated to establish a relationship between water-flow rate and boundary pressures. The experimental setup was similar to that used during the third stage[2]. The leaks that occurred in the base were resealed. Five modifications were made: (a) no bactericides were added to the water since bacteria already existed in the fractures, (b) the SAR of the water was not adjusted as during stages 1-3, (c) *m*-TFMBA at 20 ppm was used as a tracer (Table 3), (d) a flask was placed under the block to collect the outflow, and (e) two, rather than one, pressure transducers were connected to each of the two tensiometers used to measure the water pressure in the upper sand layer. The SAR was not adjusted because clay swelling was not expected to be significant since clay comprised about 1% of the total fracture coatings analyzed[2]. Two pressure transducers were used so that an average, rather than a single reading, could be used to estimate the water pressure in each tensiometer. Water flow rate into the sand was controlled using the average water pressure from the two tensiometers. The average water pressure in the middle of the sand layer was initially set at -1.0 kPa. Flow through the block continued for 17 more days.

After verifying that water continuously flowed through the block, two more modifications were made: (a) a top-loading balance was placed below the bottom flask to continuously measure the outflow rate (Figure 6), and (b) tensiometers were installed in fifteen boreholes to monitor water pressure in the fractures and matrix (three matrix

holes were not instrumented because no free channels were available on the data acquisition system). Psychrometers were not used during this stage since it was anticipated that the water potential would be close to or above the upper measurement limit of the psychrometers (-100 kPa). The latter two modifications were made over a 30-day period. The bottom pressure was not controlled; it varied throughout the sixth stage. The bottom air pressure was estimated by measuring the distance between the water meniscus in the outflow tube and the exit level in the flask (Figure 6).

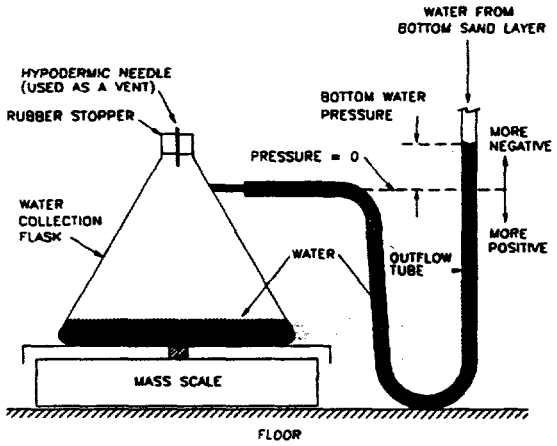

Figure 6 - Outflow collection and measuring system during stage 6.

The water was sprayed over the top sand layer for uninterrupted periods that lasted between 50 and 170 hours. The test was occasionally interrupted to service the test setup (e.g., to empty the lower water collection flask). Both data collection and water spraying were stopped during the interruptions which usually lasted between one and several hours. Water was also collected from the annulus; this service did not require an interruption.

IV. RESULTS

Two equations were used to calculate the equivalent aperture around injection holes made during stage 4; they were: (a) the ideal gas, radial and isothermal flow equation[4, p.77]:

$$k=\frac{Q_b \mu P_b \ln\left(\frac{r_e}{r_i}\right)}{\pi t\left(P_e^2-P_i^2\right)}$$

and (b) the parallel plate equation[4, p.85]:

$$k=\frac{h^2}{12}$$

Both equations were equated and solved for h = t = the equivalent pneumatic fracture aperture since the effective thickness of the injection zone, t, can not be larger than h, the fracture aperture, assuming that the matrix permeability is negligible; around hole 1E, h ≈ 100 μm; around 3A, h ≈ 200 μm, and around 4E, h ≈ 160 μm. These calculated equivalent apertures are estimates of the average aperture around the corresponding holes; they do not indicate what the distribution around each hole is.

Figure 7 shows water pressure in the upper sand layer and air pressure at the bottom outlet during stage 6. Average values of water pressure from the two tensiometers in the upper sand layer were used to control the water spraying rate. The side tensiometer (no. 2 in Figure 7) always indicated water pressure higher than that recorded by the center tensiometer (no. 1). Both tensiometers were located 5 cm above the sand-rock interface; the side tensiometer was above fracture F2, 14 cm from face 3; the center tensiometer was above the center of the block above fracture F1. As the water pressures in the upper sand layer indicate, water flow was most likely occurring through fracture F1; visually, it was less obstructed by fracture fillings than fractures F2 and F6 as seen along the top block surface. Fracture F2 did not bubble during gas injection. Water pressure increases with distance away from the sink; in this case the sink appears to be fracture F1. The temporary decreases in water pressure usually followed test interruption during which the sand became more dry as the water continued leaving the sand and entering the block.

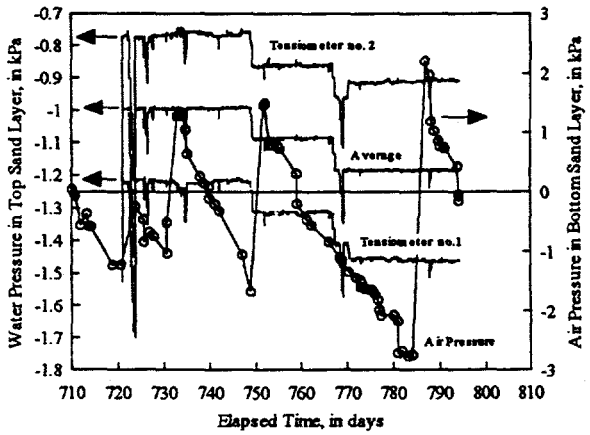

Figure 7 - Boundary pressure measurements during stage 6 [water pressure values in sand layer were made at 5 cm above top of block].

Figure 8 shows the water flow rates in and out of the block setup. The sudden increases in the input flow rate usually followed test interruptions. When spraying was stopped, water in the upper sand layer continued to flow into the block causing a decrease in the water pressure in the upper sand layer. When data collection and water spraying were resumed, the starting input flow rate was high, and gradually decreased to its pre-interruption value as the water pressure in the upper sand layer approached the desired value. Both input and output rates were about equal and showed a general decrease with time; the decrease continued even when the upper water pressure was kept steady. The output flow rate decreased considerably when pressure in the output tube became positive (days 732, 750, and 783 in Figures 7 and 8b). The decrease in output rate was not accompanied by a similar decrease in input rate indicating that water was accumulating in the block and/or in the lower sand layer. Water output resumed after the bottom air pressure decreased.

The input and output were sampled during the sixth stage for bacterial content. Input was sampled twice. Output from the lower flask and annulus was periodically sampled; these samples were from cumulative outflows that collected for several days. The bacterial content of the input water was 40,000 to 50,000 CFU/cm^3; that of the output water was between 800,000 and 1,600,000 CFU/cm^3. The prevalent species identified were *Pseudomonas spp.*, aerobic, heterotrophic, rod-shaped bacteria. Ammonium (NH_4^+) and some unidentified organic acids were detected in the outflow; they, most likely, resulted from bacterial activity in the block.

Figure 9 shows water pressure readings made by tensiometers in some of the fracture and matrix boreholes. A tensiometer is used to measure the capillary pressure (matric potential) by measuring water pressure relative to the atmospheric pressure assuming that the gas phase is continuous within the porous medium ($P_c = P_{nw} - P_w$; if P_{nw} is assumed 0, then $P_c = -P_w$). As will be shown later, this assumption was not valid for this test, and tensiometer readings did not equal capillary pressure.

Figure 9a shows water pressure in the matrix holes. Pressure in holes 2B and 3B were negative (below atmospheric pressure) throughout the observed period. The increase in pressure between days 720 and 767, and fall between days 767 and 787 in holes 2B and 3B are real rather than instrument errors since both tensiometers behaved similarly. Causes for the continuous increase and decrease in pressure are unknown. Pressure in hole 4C alternated between positive and negative values; the alternations coincided with those of the bottom air pressure

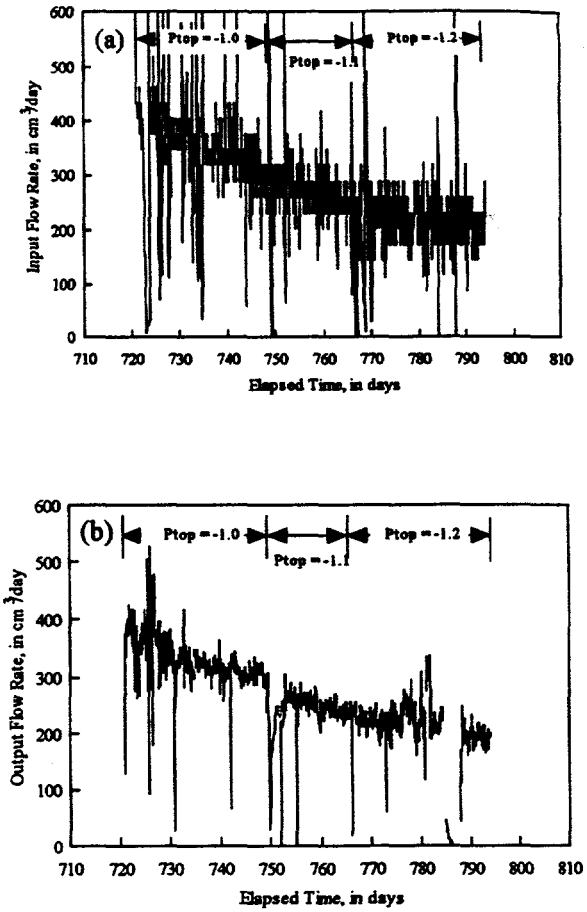

Figure 8 - Water flow rates during stage 6 at different upper boundary pressures [P_{top} = pressure along top rock-sand interface, in kPa]; (a) Inflow; (b) Outflow.

(Figure 7) inferring that this hole either communicated directly with an undetected fracture or it is very close to a fracture. This will be confirmed with future gas injection tests.

Figure 9b shows water pressure values in holes that intersected fracture F1 in the upper half of the block. Holes 1C and 1E are at about the same distance from the top; however, 1C indicated a positive pressure while 1E indicated a negative pressure. Holes 1D and 3A are at about the same level; their pressures are positive and within 0.5 kPa. Hole 1C is about 20 cm lower than hole 1D, although the difference in pressure between the two does not exceed 0.3 kPa (3 cm of water). Water pressure in hole 1E gradually decreased during stage 6, whereas the pressure in holes 1C, 1D, and 3A remained relatively constant. All pressure readings showed temporary changes that coincided with increases in the bottom air pressure.

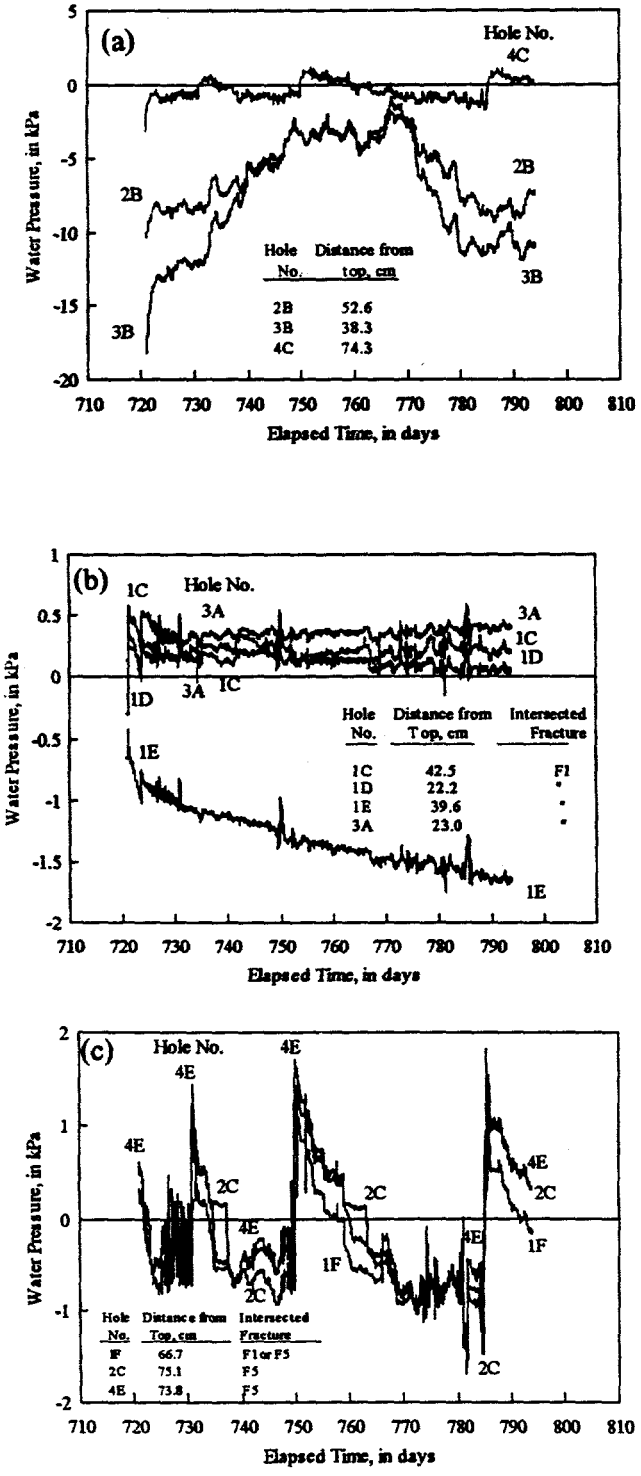

Figure 9 - Water pressure measurements within the block during stage 6. (a) matrix holes, (b) fracture holes in center of block, (c) fracture holes along block bottom.

Figure 9c shows water pressure values in fractures F1 and F5 in the lower part of the block. These water pressure values also alternated between negative and positive values and coincided with changes in the air pressure values at the bottom outlet. Hole 1F is 7 and 8 cm higher than holes 4E and 2C, respectively; hole 2C is about 1 cm lower than hole 4E. When the water pressure was positive, pressure values from holes 2C and 4E were very close; pressure in hole 1F was about 0.4 to 0.6 kPa less than the pressure in holes 2C and 4E. When pressure was negative between days 770 and 780, pressure values in all three holes were close; the pressure in hole 1F was higher than pressure in hole 2C between days 740 and 748, and days 782 and 784, even though hole 1F is 8 cm higher than hole 2C. The peak positive pressures in holes 2C and 4E reached values between 1 and 1.8 kPa; these values correspond to water accumulating in the fractures at 17 to 25 cm above bottom face of the block; no water was observed coming out of fracture traces when pressure peaks were recorded.

Figure 10 shows changes in *m*-TFMBA concentration used as a tracer during stage 6. The input concentration was kept constant at about 20 ppm. *m*-TFMBA was first detected in the annular and bottom outputs 10 days after it was introduced; both outputs were cumulative samples between days 2 and 10 after the tracer was used. The bottom output concentration gradually increased. Annular samples represent solutions that directly left the block plus water that condensed and accumulated in the annulus. Until day 720, tracer concentration in the annular water followed that of the bottom output, suggesting that most of the annular solution was from water that left the block as liquid. After day 720, concentration of the annular water decreased, indicating the amount of water that left the block from the sides as liquid was decreasing relative to the amount forming by evaporation and recondensation on the acrylic enclosure. This observation confirms that decreasing amounts of liquid water left the block from the sides even when the water pressure inside the block was positive.

V. CONCLUSIONS

Trapped gas in fractures seems to have significantly impeded water movement in the fracture network during the initial three stages; this was apparent when water did not move through fractures permeable to gas, until the gas was disturbed by the gas injection test. Fracture-wall imbibition is not likely to be the mechanism that prevented water from reaching the bottom of the block during the first four stages of this test for two reasons: (a) the fracture network is capable of continuously conducting 200 to 400 cm^3/day (Figure 8, input); on the average, this rate is much higher than the input rate observed during stage 3 (Figure 4), and (b) at the end of stage 4, parts of fractures F1 and F5 did have water even though water flow through the block did not occur. Therefore, the degree of wall-matrix

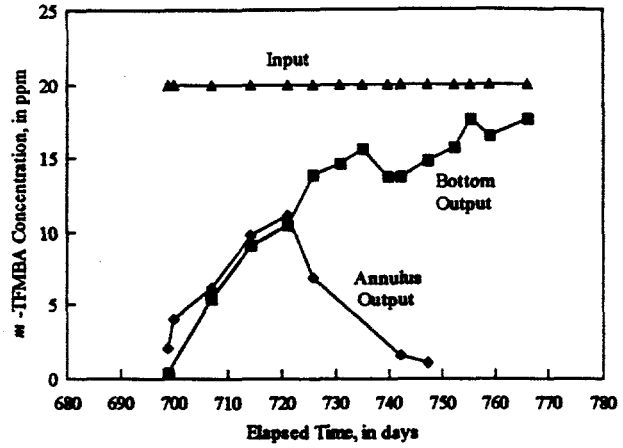

Figure 10 - *m*-TFMBA concentration in the input and output solutions.

saturation is not expected to directly impede flow; however, the amount of gas available for blockage (e.g. matrix air replaced by imbibed water) may vary depending on the saturation of the matrix surrounding a fracture. During the first three stages when the matrix was not saturated, water movement in the fractures was intermittent and sporadic. During stage 6 when the matrix was wetter, flow was continuous but not constant under the same upper boundary pressure. Subsequent experiments will continue to gradually decrease the upper pressure until flow through fracture F1 stops; then, it will be gradually increased until flow is reestablished. If flow is reestablished at a pressure less than the maximum applied during stage 3, it will indicate that entrapped gas is not as effective in impeding water movement when the matrix is nearly saturated.

The cyclic change in pressure was most likely caused by an obstruction along the bottom part of the block or in the bottom sand layer since outflow decreased or stopped when bottom air pressure increased to 1.2 to 2.2 kPa. Air blockage seems to have caused the obstruction since flow resumed repeatedly (non-permanent blockage). An explanation to the oscillating behavior may be: when air gets entrapped it decreases the area available for water to flow, thus reducing the permeability to water; once air forms a continuous phase across a section in the porous medium, water flow will stop, and will not resume unless the air is pushed away from the water path; air can not be removed until the liquid pressure exceeds the minimum air entry pressure in the blocked section. Based on the maximum water pressures reached at the bottom of the block prior to clearing the obstruction (1.7 to 2.5 kPa), air blockage may have been occurring in the lower sand layer since the sand has an air entry pressure close to the pressure required to clear the obstructions (Figure 3). The oscillatory behavior may be an experimental artifact; however, an obstruction also was observed during the first three stages when the lower sand layer was dry. The periodic blockage in outflow did not change long-term trends where outflow rates appeared to continue trends prior to the blockages. The top water pressure during stage 3 was increased to 1.4 kPa without achieving continuous flow into the block; this pressure is less than 1.7 kPa. Had the top water pressure been increased to a values between 1.7 and 2.5 kPa, water might have overcome air blockage and entered the fractures.

During the first two stages, water flow rate into the block significantly decreased[2] when the water pressure at the sand-rock interface above fracture F1 decreased to -0.75 kPa; the equivalent outer hydraulic aperture of fracture F1 along the top was estimated at 200 μm based on the capillary rise formula for parallel plates. During stage 6, water continued to flow into fracture F1 even when the pressure at the sand-rock interface became less than -1 kPa (Figure 7, tensiometer no. 1); the equivalent hydraulic aperture at this pressure is estimated to be smaller than 150 μm. The aperture along the sand-rock interface can not be estimated until the pressure at which water stops entering fracture F1 is reached; such measurements are underway. Equivalent fracture aperture calculated from the capillary rise formula (200 μm) was close to pneumatic apertures calculated from the gas injection test (100 to 200 μm).

Another known cause of variations in water permeability is bacterial growth[5]. Since the bacteria identified in this test were aerobic, they are not expected to have produced gas. Bacterial activity may influence permeability by other mechanisms such as physical plugging and slime production which may change rock wettability[5]; however, no measurements were made during this experiment to test for any bacterial effects. The long-term decrease in the outflow rate may have been caused by bacterial activity; this will be verified in a successive test.

Water pressure measurements in Fracture F1 were different at points with almost same elevation. The difference in pressure between holes was not accounted for by differences in elevation. These anomalies indicate the formation of flow channels within the same fracture, accompanied by aperture variations.

The upper boundary water pressure was controlled during the test; the bottom pressure was not controlled. The air pressure cycled about zero (atmospheric pressure) several times. When the bottom air pressure became positive, water accumulated in the fractures. Several tensiometers in the middle part of the block indicated positive water pressure throughout stage 6 of the test. In all

s where a positive pressure was observed, no water seen coming out of the fractures along the block sides. cyclic air pressure behavior along the bottom sand and water accumulation in the fractures along the om part of the block infer that air in the lower sand and/or fractures was isolated from the atmospheric air. nentioned earlier, to measure the capillary pressure a tensiometer, the assumption that the air phase is inuous with the atmosphere is made; this assumption not valid in this test. Therefore, if $P_c = P_{nw} - P_w$, and $_{nw}$ is unknown, then P_c is unknown.

The tensiometer probes developed for this study appear quate to measure water pressure in fractures. The same nique can be used in the field experiment. As ntioned above, to measure matric potential, the air ssure in the fractures also needs to be measured in ations close to tensiometer measuring points; further earch needs to be conducted on this measurement.

A relation between boundary pressures and flow rate s not achieved since the inflow and outflow rates ough the block did not stabilize. No sharp changes in w rates were observed when the upper boundary ssure was changed; this may be an artifact of the system h two surrounding sand layers with relatively high rativity rather than a true behavior of fracture flow. The tflow rate continued to decrease even when the average ssure along the upper boundary was kept steady; this y have been caused by a continuous formation of air ocks in the fractures and/or the sand layers. Bacterial tivity also may have caused continuous changes in rock operties along the fracture walls.

OMENCLATURE

FU	colony-forming units
	fracture aperture
)	inside diameter
	permeability
-TFMBA	meta-trifluoromethyl benzoic acid
$_b$	base (reference) pressure
$_c$	capillary pressure
$_e$	pressure at external boundary
$_i$	pressure at internal boundary
$_{nw}$	pressure of non-wetting phase
$_w$	pressure of wetting phase
)pm	parts per million (by mass)]
Q_b	volumetric flow rate measured at P_b
$_e$	radius to external boundary
$_i$	radius to internal boundary
S_w	saturation of water
SAR	sodium adsorption ratio
std	standard deviation of sample
t	thickness of injection zone
T_0	time when data acquisition started (25-Oct-91)
μ	viscosity

REFERENCES

1. U.S. Department of Energy, *Site Characterization Plan, Yucca Mountain Site, Nevada Research and Development Area, Nevada*, Nuclear Waste Policy Act (Section 113), vol. IV, Part B, Ch. 8, Sec. 8.3.1.2.2.4.2, December (1988).

2. F. Thamir, E.M. Kwicklis, and S. Anderton, "Laboratory Study of Water Infiltration into a Block of Welded Tuff", *Proceedings of the 4th Annual International High-Level Radioactive Waste Management Conference*, April 26-30, 1993, p. 2071-2080, American Society of Civil Engineers, Las Vegas, Nevada, (1993).

3. L.E. Allison, "Effect of Microorganisms on Permeability of Soil Under Prolonged Submergence", *Soil Science*, vol. 63, p. 439-450, (1947).

4. J.W. Amyx, D.M. Bass Jr., and R.L. Whiting, *Petroleum Reservoir Engineering, Physical Properties*, McGraw-Hill Book Co., New York, (1960).

5. P. Vandevivere and P. Baveye, "Saturated Hydraulic Conductivity Reduction Caused by Aerobic Bacteria in Sand Columns", *Soil Science Society of America Journal*, vol. 56, p. 1-13, (1992).

DISCLAIMER

HIGH LEVEL RADIOACTIVE WASTE MANAGEMENT

Proceedings of the Fifth Annual International Conference Las Vegas, Nevada, May 22-26, 1994

VOLUME 1
1994

Sponsored by the
American Society of Civil Engineers
American Nuclear Society

in cooperation with:

American Association of Engineering Societies
American Chemical Society
American Institute of Chemical Engineers
American Medical Association
American Society for Testing and Materials
American Society for Quality Control
American Society of Mechanical Engineers
Center for Nuclear Waste Regulatory Analysis
Edison Electric Institute
Geological Society of America
Health Physics Society
Institute of Nuclear Materials Management
National Conference of State Legislatures
Society of Mining Engineers
U.S. Department of Energy
U.S. Geological Survey
U.S. Nuclear Regulatory Commission
University of Nevada Medical School
American Institute of Mining, Metallurgical and Petroleum Engineers
American Underground-Space Association
Atomic Energy Council Radwaste Administration
Atomic Energy of Canada Ltd.
British Nuclear Fuels Ltd.
Chinese Institute of Civil and Hydraulic Engineering
Commission of the European Communities
Conseil National des Ingenieurs et des Scientifiques de France
Electric Power Research Institute
Her Majesty's Inspectorate of Pollution
Hungarian Nuclear Society
Institution of Civil Engineers
Institution of Engineers-Australia
Institution of Engineers of Ireland
Japan Society of Civil Engineers
Korea Advanced Energy Research Institute
Korean Society of Civil Engineers
Ministerio de Industria y Energia-Uruguay
National Association of Corrosion Engineers
National Association of Regulatory Utility Commissioners
Nationale Genossenschaft fur die Lagerung Radioaktiver Abfalle (NAGRA)
National Society of Professional Engineers
Organization for Economic Cooperation and Development (OECD)- Nuclear Energy Agency
Power Reactor and Nuclear Fuel Development Corp.
Romanian Nuclear Energy Association
Swedish Nuclear Fuel and Waste Management Company
Swedish Nuclear Power Inspectorate
Swiss Society of Engineers and Architects
U.S. Council for Energy Awareness
Verein Deutscher Ingenieure

Hosted by
University of Nevada, Las Vegas
Howard R. Hughes College of Engineering

Published by the

American Nuclear Society, Inc.
La Grange Park, Illinois 60525, USA

American Society of Civil Engineers
345 East 47th Street
New York, New York 10017-2398, USA